Cold Spring Harbor Symposia on Quantitative Biology

Drosophila Brain Development: Closing the Gap between a Macroarchitectural and Microarchitectural Approach

A. Cardona, S. Saalfeld, P. Tomancak, et al.

Cold Spring Harb Symp Quant Biol published online December 22, 2009
Access the most recent version at doi:10.1101/sqb.2009.74.037

Drosophila Brain Development: Closing the Gap between a Macroarchitectural and Microarchitectural Approach

A. CARDONA,[1,2] S. SAALFELD,[3] P. TOMANCAK,[3] AND V. HARTENSTEIN[1]

[1]*University of California at Los Angeles, Department of Molecular Cell and Developmental Biology, Los Angeles, California 90095;* [2]*Institute of Neuroinformatics, Uni/ETH Zurich, CH-8057 Zurich, Switzerland;* [3]*Max-Planck Institute for Cell Biology and Genetics, Dresden, Germany*

Correspondence: volkerh@mcdb.ucla.edu

Neurobiologists address neural structure, development, and function at the level of "macrocircuits" (how different brain compartments are interconnected; what overall pattern of activity they produce) and at the level of "microcircuits" (how connectivity and physiology of individual neurons and their processes within a compartment determine the functional output of this compartment). Work in our lab aims at reconstructing the developing *Drosophila* brain at both levels. Macrocircuits can be approached conveniently by reconstructing the pattern of brain lineages, which form groups of neurons whose projections form cohesive fascicles interconnecting the compartments of the larval and adult brain. The reconstruction of microcircuits requires serial section electron microscopy, due to the small size of terminal neuronal processes and their synaptic contacts. Because of the amount of labor that traditionally comes with this approach, very little is known about microcircuitry in brains across the animal kingdom. Many of the problems of serial electron microscopy reconstruction are now solvable with digital image recording and specialized software for both image acquisition and postprocessing. In this chapter, we introduce our efforts to reconstruct the small *Drosophila* larval brain and discuss our results in light of the published data on neuropile ultrastructure in other animal taxa.

Studies of nervous system architecture and function typically approach the brain at two different levels of resolution: macrocircuitry and microcircuitry. The macrocircuitry-oriented approach asks these questions: What functions can be attributed to brain compartments such as the mammalian primary visual cortex or lateral geniculate nucleus and what is the connectivity between these and other brain compartments? In contrast, the study of microcircuitry zooms in on neurons, their dendrites, axons, and synapses. Thus, the way in which a given neuron is tuned to a specific input stimulus, or the pattern of activity triggered in this neuron when providing a specific input, depends on the distribution of excitatory and inhibitory synapses that connect the neuron with its neighbors (Douglas and Martin 1998; Silberberg et al. 2002; Toledo-Rodriguez et al. 2005; Silberberg 2008). The analysis of microcircuits is of great importance. All acts of fine motor control, memory formation, and cognition can only be understood if the microcircuitry within the brain compartments dealing with these functions is known. Likewise, the insight into psychiatric disease mechanisms and their pharmacological treatment requires that brain microcircuitry be known. For example, recent findings suggest that diseases such as schizophrenia can be understood in terms of abnormalities in the microcircuitry of the prefrontal cortex (Winterer and Weinberger 2004; Rolls et al. 2008).

This useful conceptualization of the nervous system as being composed of interconnected, structurally defined compartments, constituting microcircuits integrated into macrocircuits, also applies to the brain of invertebrates, such as the fruit fly *Drosophila*. The nervous system of *Drosophila* (and insects in general) is formed by a relatively small number of genetically and structurally defined modules, the neural lineages. The ventral nerve cord and subesophageal ganglion (containing the circuits controlling locomotion, flight, and feeding) are built of ~80 bilaterally symmetric pairs of lineages; the central brain, a mostly sensory and associative center, is formed by 100 paired lineages (Goodman and Doe 1993; Younossi-Hartenstein et al. 1996; Urbach and Technau 2003; Truman et al. 2004). Each lineage is derived from an asymmetrically dividing stem cell, called the neuroblast, that is born in the early embryo (Fig. 1A) (Hartenstein et al. 2008a,b). Neuroblasts and the lineages they produce represent genetic modules ("units of gene expression"). The expression pattern of more than 40 transcription factors in specific embryonic neuroblasts has been described previously (Urbach and Technau 2003). A given transcription factor becomes active in one, or a small number of, neuroblasts; a particular neuroblast thereby acquires a "genetic address," consisting of a specific set of transcription factors active in this cell. It is thought that this genetic address will essentially be involved in shaping the morphology and function of the lineage of neurons produced by the neuroblast.

Lineages also form structural modules. Thus, neurons that belong to one lineage remain together throughout development, forming compact clusters of cells (Fig.1B). More importantly, axons emitted by neurons of one lineage also form a coherent fascicle, the primary and secondary lineage axon tracts. This means that neurons of

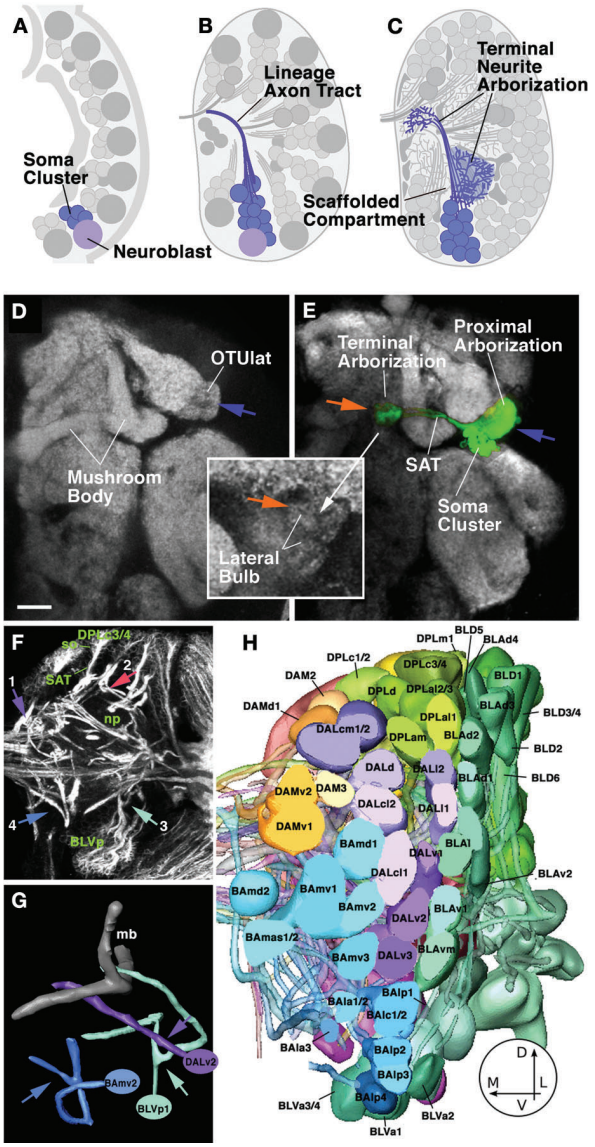

Figure 1. Developmental and structural characteristics of wild-type lineages. (*A–C*) Lineages as units of gene expression, projection, and connectivity. Stereotyped population of neuroblasts generates neurons in the embryo and larva (*A*). Neurons belonging to one lineage form a cohesive cluster and project their axons in one fascicle (*B*). Terminal branches of neurons of one lineage arborize in specific neuropile compartments (*C*). (*D,E*) Z-Projection of adult brain hemisphere labeled with anti-Bruchpilot (Nc82; Kittel et al. 2006) to visualize neuropile compartments (white). (*E*) One lineage, DALcl1, is labeled by expression of green fluorescent protein (GFP). Note dense proximal arborization restricted to lateral domain of optic tubercle (OTUlat; one of the optic foci); distal arborization is restricted to the lateral bulb, one of the input regions of the central complex. (*F*) Z-Projection of 10 successive 1-µm confocal cross sections at the level of the central neuropile. Secondary lineages, their axon tracts (SATs), and neuropile fascicles formed by convergence of SATs are labeled with antineurotactin antibody (white). Clusters of somata (so) belonging to lineages are located in the cortex; axon tracts project centripetally into the neuropile (np). Arrows point at lineages representing the types of SAT trajectories observed: SAT is unbranched and enters the neuropile in a straight course (*1*; DPMm lineage) or after a sharp turn at the cortex–neuropile boundary (*2*; DPLc3/4). (*3*) SAT bifurcates into two branches at cortex–neuropile boundary (BLVp1/2); (*4*) distal part of SAT bifurcates in neuropile (BAmv2). (*G*) Digital models of three representative lineage tracts illustrating typical branching behavior of SATs (DALv2: straight unbranched entry into neuropile; BLVp1: bifurcation at point of entry into neuropile [arrowhead]; BAmv2: bifurcation in distal leg of SAT). (*H*) Three-dimensional digital models of all clusters of neuronal somata representing all lineages of one brain hemisphere (anterior view). The polar region of the cortex was removed for a clearer view of lineages. Bar, 20 µm. (*F–H*, Modified from Fung et al. 2009 [©Elsevier].)

one lineage share their principal trajectory; they form a "unit of projection" (Fig.1C–G). Lineages thereby represent the most appropriate structural/developmental units of brain macrocircuitry. On the basis of their characteristic location and axon tract, we have generated an atlas of all lineages of the central brain for the larval stage (Fig. 1H) (Pereanu and Hartenstein 2006). Attempts are currently under way to link the larval lineage map with the adult stage, when each lineage has completed its terminal arborization (Pereanu et al. 2009).

We briefly summarize our recent findings pertaining to the structure and development of neural lineages of the *Drosophila* brain. We then outline our approach to reconstruct microcircuitry in the fly brain using computer-aided serial electron microscopy, an approach that is guided by the lineage-centered macroarchitectural map of the fly brain. Finally, we describe first results shedding light on *Drosophila* microcircuitry and discuss these data in the context of brain evolution.

LINEAGE-BASED ANALYSIS OF *DROSOPHILA* BRAIN STRUCTURE AND DEVELOPMENT

Using clonal marking techniques and specific Gal4 driver lines (Brand and Perrimon 1993), we have analyzed representative *Drosophila* brain lineages at all stages of development (Larsen et al. 2009). Most lineages have a number of important characteristics in common; our focus was on these generic lineage features. The early neurons of a lineage generated during embryogenesis (primary neurons; 15–20 neurons per neuroblast for the large majority of lineages) stay together as a coherent cluster (Fig. 2A,B). Likewise, axons of each lineage form a coherent bundle (primary axon tract [PAT]) that follows a stereotyped pathway in the neuropile (Younossi-Hartenstein et al. 2006). Apoptotic cell death removes an average of 30%–40% of neurons from the primary lineages around the time of hatching. Secondary neurons generated later, during the larval period, also form clusters that stay together all the

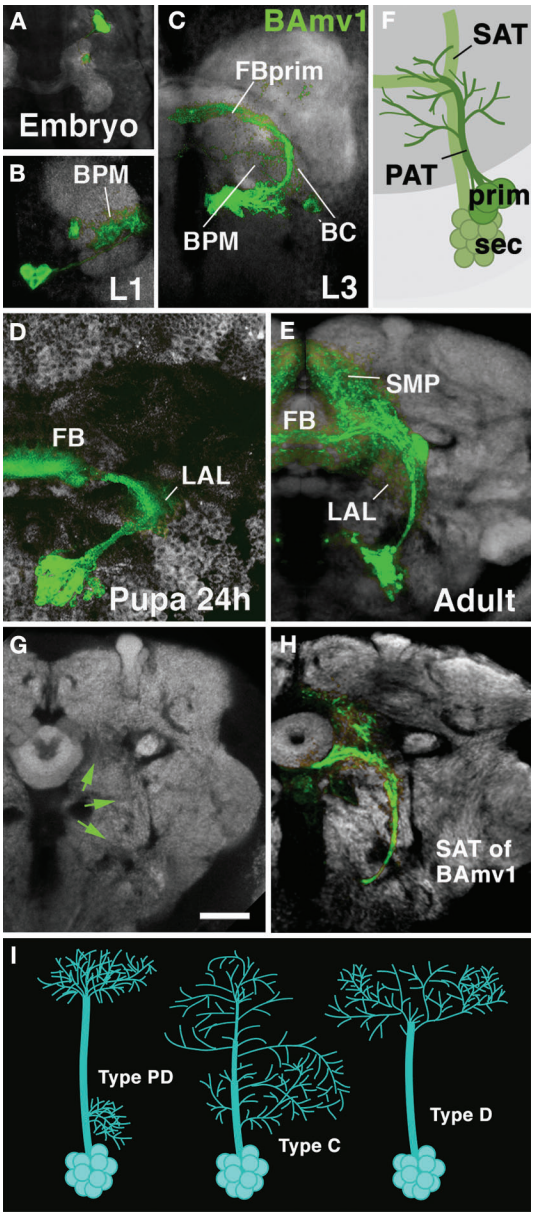

Figure 2. Morphogenesis of a brain lineage from embryo to adult. (*A–E*) Z-Projections of confocal sections of one brain hemisphere in which BAmv1 lineage is labeled by GFP driven by the line *per*-Gal4 (Kaneko and Hall 2000). BAmv1 has a conspicuous crescent-shaped tract, projecting first posteriorly, then dorsolaterally, and finally dorsomedially toward the primordium of the fan-shaped body (FBprim), which forms part of the CPM compartment of the larval brain. Arborizations of primary neurons occur in BC, BPM, and FBprim compartments (*B,C*). Secondary axons follow the same trajectory and branch in the lateral accessory lobe (LAL), fan-shaped body (FB), and superior medial protocerebrum (SMP; *D,E*). (*F*) Schematic illustrating that SAT typically fasciculates with, or at least grows close to, PAT of the corresponding lineage. (*G,H*) Secondary axon tracts develop into long fiber bundles of adult brain. (*G*) Frontal confocal section of adult brain hemisphere labeled with anti-Bruchpilot (Nc82; neuropile; white). (*H*) Secondary neurons of the BAmv1 lineage are labeled by GFP (driven by *per*-Gal4). Note that the coherent secondary axon tract of BAmv1 now forms a long fiber bundle that is visible as a Nc82-negative (i.e., synapse-free) "tunnel;" indicated by green arrows (*G*). (*I*) Schematic representation of different types of lineages encountered in *Drosophila* brain (PD, separate proximal and distal arborization; C, continuous arborization; D, distal arborization). Bar, (*G*) 20 µm (all photographic panels at same scale).

way to the adult stage and that form cohesive axon bundles (secondary axon tract [SAT]). SATs project into the neuropile compartment visited by the corresponding primary axon tract (Fig. 2C,F). SATs develop into the long fiber fascicles that interconnect the different compartments of the adult brain (Fig. 2D,E). These fascicles can be easily recognized by labeling brains with global markers. For example, labeling with synaptic markers such as the anti-DNcad or anti-Brp antibody fascicles (which only contain long fibers and lack synapses) stand out as signal negative channels (Fig. 2G,H).

With respect to overall arbor geometry, we distinguish between three types of lineages (Fig. 2I) (Larsen et al. 2009): Type-PD ("proximodistal") lineages are characterized by distinct, spatially separate, proximal (close to soma) and distal arborizations; type-C ("continuous") lineages have arborizations distributed more or less evenly along the entire length of their tract; and type-D lineages ("distal") lack proximal arborizations (their fiber tract extends for a considerable distance into the neuropile before branching into a more or less complex distal arbor).

Arborizations of lineages, in particular those of type PD, are restricted to distinct neuropile compartments; we propose that compartments are "scaffolded" by individual lineages or small groups thereof. Primary lineages set up the compartment map already in the embryo. Compartments then grow during the larval period simply by an increase in arbor volume of primary neurons. Arbors of secondary neurons form within the larval compartments, resulting in smaller compartment subdivisions and additional, adult-specific compartments. We proposed that each compartment has its own "scaffolding lineage" (or set of scaffolding lineages) that would be defined in the following manner. (1) During development, the outgrowth of neurites from a line-

age S generates the compartment S′. If S is deleted, S′ also does not form; this has been shown for the calyx, the compartment scaffolded by the four MB (mushroom body) lineages (Ito et al. 1997), and for compartments of the central complex (JK Lovick and V Hartenstein, unpubl.). (2) The arborization of lineage S forms a dense matrix of terminal fibers on which synapses of S neurons themselves, as well as extrinsic neurons that enter compartment S′ from the outside, are made. Again, the calyx provides an example in this case: Electron microscopy (EM) investigations have shown that the majority of the postsynaptic terminal neurites belong to neurons of the MB lineages (Yasuyama et al. 2002). Our lab and others have found numerous other lineages whose proximal (or sometimes distal, axonal) terminal arborizations, in the adult brain, are highly focused in a small compartment. As an example in point, Figure 1, D and E, shows the labeled lineage DALcl1 with dense terminal arborizations in a small subcompartment, the lateral optic tubercle (OTUlat), and terminal arborizations confined even more narrowly to the lateral bulb, an input region of the central complex.

In summary, our data support the idea that lineages form the developmental/anatomical substrate of *Drosophila* brain macrocircuitry: Compartments and the long axon tracts interconnecting them can be assigned to specific (sets of) lineages. The reconstruction and digital representation of all lineages, including their axonal and dendritic arborization and interconnecting axon fascicle, will add up to a complete map of fly brain macrocircuitry.

ANALYSIS OF MICROCIRCUITRY

The anatomical reconstruction of microcircuitry requires the documentation of, at the level of single synapses and neuronal processes, how neurons in a given (small) volume of the brain are interconnected. Due to their small size, which lies in the range of 0.1–0.5 µm, fine neurites and their synaptic contacts can be conclusively shown only electron microscopically. However, the acquisition of complete series of EM sections and their photographic documentation and analysis requires a considerable effort, and therefore, studies of microcircuitry have traditionally been restricted to small parts of neurons or neuropile compartments in insects or other invertebrates (see, e.g., Watson and Burrows 1983; Meinertzhagen and O'Neil 1991; Yasuyama et al. 2002). The relatively complete reconstruction of the miniature *Caenorhabditis elegans* central nervous system, containing less than 400 unbranched neurons, represents a notable exception (White et al. 1986). The problem of image acquisition and reconstruction is now solvable with digital image recording and specialized software for image acquisition and postprocessing, and we and other groups have begun to generate stacks of digitized images from serial EM sections. These stacks can be segmented and analyzed in their entirety, which makes it possible to reconstruct the way a neuron (or neurite) is connected to its immediate neighbors.

It should be pointed out that even with the digital technology available today, digital serial EM-based analysis is still feasible only for relatively small objects in the millimeter range. That means that for a large vertebrate brain, only small "aliquots" of brain tissue can be processed. But this may be sufficient if one assumes (and evidence for this assumption is accumulating; for review, see Kozloski et al. 2001; Silberberg et al. 2002) that large brain areas such as the neocortex are essentially built in a stereotypical manner; this means that the microcircuitry characteristic of one cortical area is highly similar to that in a different area, and thus many of the principles of microcircuitry that emerge from the analysis of one tissue "aliquot" can be generalized to other cortical domains. In our view, this concept does not argue against location-specific properties. It merely suggests that it is practical to first undertake a comprehensive analysis of stereotyped aspects of microcircuitry; this then will make it easier to get at additional site-specific properties.

Insect brains offer the advantage of a much smaller size. The early first instar larval (L1) brain of *Drosophila*, formed by ~1500 differentiated and functional nerve cells (Larsen et al. 2009), has a diameter of ~50 µm. The neuropile that forms the center of a brain hemisphere measures less than 30 µm. Given these specifications, we are currently working with ~500 sections of 60-nm thickness; a more complete series of sections that includes both brain hemispheres and the ventral nerve cord is under way. We aimed at a resolution of ~2–3 nm per pixel; synaptic contacts and fine processes (diameter of ~100 nm), or even synaptic vesicles (20–30 nm), can be clearly resolved at this resolution. The size of the digitized image of one section contains ~15,000 × 15,000 pixels. We have packed the entire postprocessing pipeline in our own custom software TrakEM2, which is based on ImageJ, a National Institutes of Health (NIH)–sponsored image processing platform (www.ini.uzh.ch/~acardona/trakem2.html). The software allows us to stitch individual photographs covering one section into one seamless montage, to register montages of each section, and to navigate the resulting stack of sections efficiently (Saalfeld et al. 2009; Cardona et al., unpubl.).

MICROCIRCUITRY DATA ANALYSIS AND RECONSTRUCTION: MERGING EM AND LM DATA

When browsing EM sections, the staggering amount of data collected becomes very difficult to process without a priori "low-resolution knowledge" of the architecture of the object, i.e., the L1 *Drosophila* brain. The navigation of TEM (transmission electron microscopy) images must be guided by known, labeled, and registered confocal stacks that provide cues regarding the position of major "macroarchitectural" landmarks such as axon bundles or neuropile compartment boundaries, thus providing the necessary context for the analysis of microarchitectural components of the neuropile. In other words, if users want to zoom in on the pattern of connectivity in a small volume of neuropile, they need to know the compartment in which this volume is located in or the lineages and major tracts that connect the compartment to the rest of the brain. The TrakEM2 pipeline is designed to embed the analysis of the EM stack at the microcircuit level into the light-microscopically derived macroarchitectural framework.

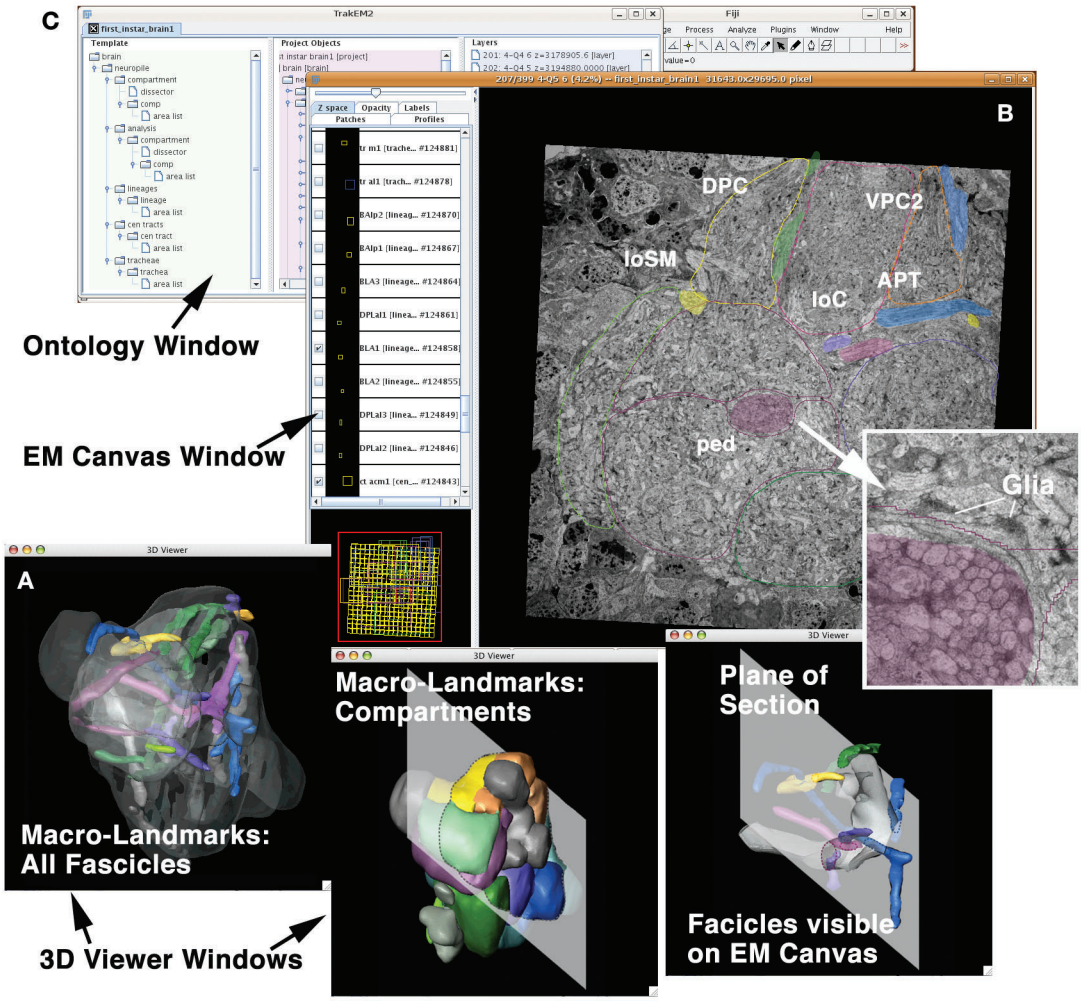

Figure 3. Graphical user interface of TrakEM2. The EM canvas presents the EM stack. The user can scroll and navigate through all sections in the "Google Map" style. Identified structures (e.g., compartments and lineage tracts) can be segmented. The ontology window displays all segmented objects as a hierarchically organized list. The interactive 3D viewer windows show selected objects segmented from the EM stack.

We have defined a set of lineages, compartments, and major axon tracts that can be recognized at all developmental stages in the adult and that serve as macroarchitectural landmarks. In our preliminary L1 EM stack, we could identify most of these landmarks, including compartments, neuropile fascicles, and individual lineage tracts (Fig. 3A). Thus, the lineage-associated primary axon tracts of the L1 brain contain 6–20 tightly bundled, straight axons that are visible in the EM stack if one knows where to look for them (Fig. 3B). Moreover, PATs of multiple lineages converge to form major axonal "thoroughfares" in the neuropile, such as the antennocerebral tract, peduncle, or longitudinal central tract. These tracts are all associated with high concentrations of glial processes that further facilitate their recognition in the EM stack. Glial densities also define many of the compartment boundaries (Younossi-Hartenstein et al. 2003). After identifying and segmenting the macroarchitectural landmarks in the EM stack, they become the objects of an intrinsic macromodel. Thus, with the help of the drawing tool, label fields are created on each section; the label fields stacked along the *z* axis form a given object for which a surface is generated and which can be displayed as an interactive digital three-dimensional (3D) model.

Figure 3 shows the current graphic user interface of TrakEM2. It is composed of three simultaneously active windows: the ontology window (Fig. 3C), EM (raw data) canvas (Fig. 3B), and 3D viewer windows (Fig. 3A). All objects of the model are displayed as a hierarchical list in the ontology window; here, individual objects can be activated or inactivated, and properties of the digital rendering of each object, such as color or transparency, can be changed. Activating an object in the ontology window will lead to its appearance in the EM canvas window, as well as in the 3D viewer. In both EM canvas and 3D viewer windows, one can further interact with the object in manifold ways. As a result, TrakEM2 allows us to focus on any part of the neuropile in the EM canvas and, at the same time, look up in the intrinsic macromodel (displayed in the 3D viewer) where we are and the lineages or tracts that are close by.

QUANTITATIVE ANALYSIS OF CONNECTIVITY IN "MICROVOLUMES"

Given that the problems of sectioning, EM imaging, and data handling of complete L1 brains are in principle solved, our ultimate goal is to reconstruct all neurons and their connections in their entirety. However, even a complete stack without any gaps will be difficult to register "perfectly" in toto, given the current technology. "Perfectly" would imply that, given the thinness of terminal processes, any pixel of the 15,000 x 15,000 pixel montage has to be <25 pixels (≅100 nm) removed from its "true" *x/y* position. Considering the fact that sectioning, heating (electron beam), and handling add up to deformations of all sections (independent of one another), it will be understandable that it is currently impossible to register section montages with that accuracy. The strategy is therefore to break down the overall EM stack volume into smaller "microvolumes," in the range of 5 x 5 x 5 µm, and reconstruct these. TrakEM2 allows us to efficiently "cut out" microvolumes from the total stack and reregister them automatically, as well as manually, at an accuracy level high enough for segmenting even fine processes. Multiple microvolumes can be sampled from any desired position, guided by the macrolandmarks. It should be noted that, even irrespective of the technical factors that suggest the microvolume approach, this approach seems also to be conceptually well justified. Thus, as pointed out for the vertebrate brain above, it stands to reason that the *Drosophila* brain is structured in a stereotypical way: The biological "algorithm" underlying the neuronal wiring in a given microvolume may well resemble that of a neighboring volume. It seems appropriate to sample and compare microvolumes from different compartments, formed by different lineages and reached by different types of sensory inputs, before eventually reconstructing the entire neuropile in toto. The following fundamental parameters of microcircuitry can be gained from the microvolumes:

- Types of neurites (diameter, shape, branching behavior) that exist.
- Density/directionality of neurites (of different types) within a microvolume.
- Density of branchpoints and how branching of different neurites is coordinated.
- Density and distribution of input/output synapses, relative to neurite type, neurite directionality and branching behavior.

In the following section, we summarize our recent findings (Cardona et al., unpubl.) that have begun to provide information regarding these parameters.

DROSOPHILA BRAIN MICROCIRCUITRY: NEURITE PROFILES AND DISTRIBUTION OF SYNAPSES

The brain neuropile contains neurites connected by synapses, as well as glia. Recognizable by their lamellar shape and high electron density, glial processes form more or less continuous sheaths around the neuropile surface, as well as around many compartments and fascicles. Within neuropile compartments, fine glial processes are interspersed with terminal neurites and synapses. Neurites come in several different classes that relate in a systematic way to presynaptic and postsynaptic contact sites (Fig. 4). We distinguish among axiform, varicose, globular, and dendritiform neurites (Fig. 4A–C). These generic classes of neurites can be found in all compartments of the brain. Axiform neurites (axis = axle) are straight, unbranched processes of even diameter, ranging between 0.2 µm and 0.4 µm. These processes typically form bundles. The PAT emitted by the neurons belonging to one lineage consists of axiform neurites. Within the neuropile, thick bundles of axiform neurites (created by the coalescence of multiple PATs) form the long fiber tracts, such the antenno–protocerebral tract. Varicose neurites (varix = dilated vein) comprise most of the volume of the neuropile. They represent branched processes that vary in diameter and change direction. Along their length, thin segments (0.2–0.4 µm) alternate with swellings ("varicosities") that measure 0.5–1.5 µm. Globular neurites (globus = round body) contain one (terminal) or several large diameter (1.5–3 µm) round or irregularly shaped segments. These formations structurally and functionally resemble closely the end plates, or "boutons," of motor axons. Dendritiform neurites (dendron = tree) are thin, highly branched processes. They change direction frequently. Short, terminal branches of these "trees" are in the range of 0.1 µm.

Synapses are defined by the characteristic presynaptic site, an electron-dense patch of membrane bordered by the T bar, a cytoplasmic specialization involved in tethering and docking of synaptic vesicles (Fig. 4D) (Feeney et al. 1998; Kittel et al. 2006; Prokop and Meinertzhagen 2006). Synaptic vesicles can be observed at or near presynaptic sites. Presynaptic contact sites are relatively uniform in size, ranging from 0.1 µm to 0.3 µm, and are very predominantly found on large-diameter segments of neurites, i.e., the swellings of varicose and globular neurites (Fig. 4E); these neurites then constitute the output, or axonal, branches within the neuropile. Postsynaptic sites are less conspicuous membrane densities lacking T bars or synaptic vesicles; they are found almost exclusively on thin dendritiform neurites and, occasionally, thin side branches of varicose neurites. The discrepancy in diameter between presynaptic and postsynaptic neurites naturally creates the characteristic polyadic synapse: The relatively large size of the presynaptic element creates a "platform" that is in direct contact with multiple, thin, postsynaptic elements (Fig. 4D). It should be noted that for most synapses, it is difficult to infer exactly how many postsynaptic partners exist. Thus, postsynaptic membrane specializations are very subtle, and one can only base the assertion that a given profile represents a postsynaptic partner on whether its membrane is in direct contact with the presynaptic membrane (density). This, in numerous cases, is ambiguous (e.g., Fig. 4D).

In vertebrates, neurons show three different compartments: soma, dendrite, and axon (Fig. 4F). Dendrites arise from the soma and in terms of structure (e.g., microtubule

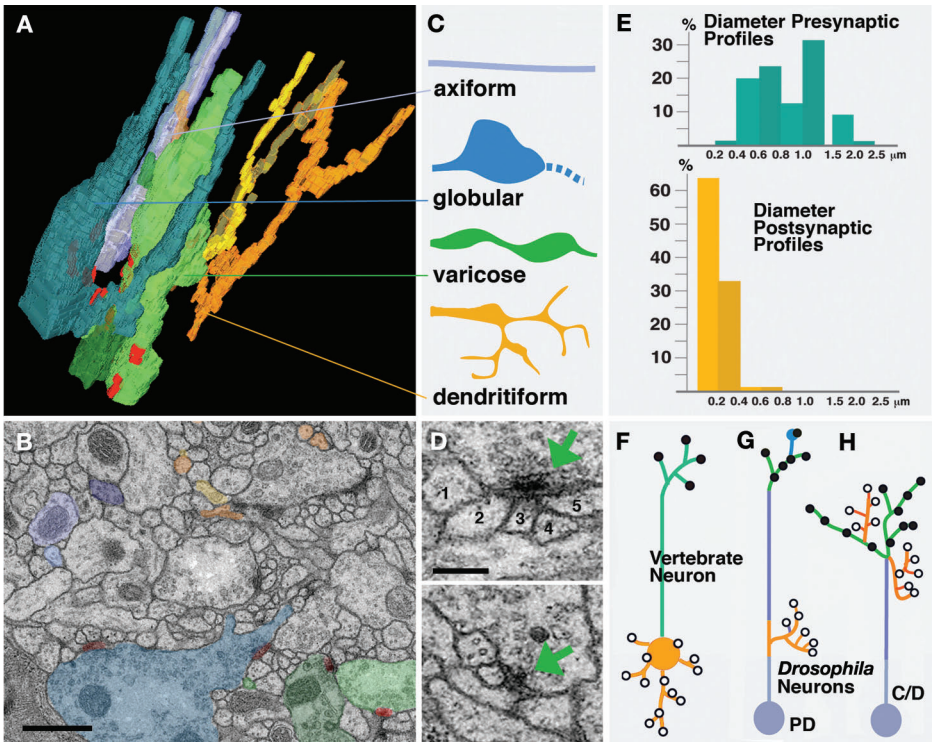

Figure 4. *Drosophila* neuropile ultrastructure. (*A–C*) Types of neurite profiles. (*A*) Three-dimensional digital model of several short neurites segmented from one microvolume. (*B*) Representative EM section of microvolume in which profiles of neurites modeled in *A* are shaded in the corresponding colors. (*C*) Schematic depiction of types of neurites. Axiform neurites (light blue) are straight unbranched processes of intermediate (0.2–0.4 µm) diameter. Globular neurites and varicose neurites (dark blue and green) have alternating segments of intermediate (0.2–0.4 µm) and large (0.5–1.5 µm for varicose; 1–3 µm for globular neurites) diameter. Dendritiform neurites (yellow, brown, orange) are highly branched and thin (<0.2 µm). (*D*) Section of two typical polyadic synapses. (Green arrow) Presynaptic specialization, consisting of the T bar and synaptic vesicles. Presynapses are contacted by multiple, thin branches of dendritiform processes. Numbers *1–5* in upper panel denote profiles of thin, postsynaptic profiles (dendritiform neurites); *2–5* have clear direct contact to presynaptic zone; *1* is located adjacent to the presynaptic site and represents a case that may represent a postsynaptic neurite of this synapse. (*E*) Correlation between frequency of presynaptic and postsynaptic sites and neurite diameter. Presynaptic sites (blue; *top*) are found predominantly on large-diameter profiles that correspond to thick segments of varicose and globular neurites. These neurites represent terminal axonal branches. Postsynaptic profiles (yellow, *bottom*) almost exclusively belong to thin dendritiform neurites; they represent terminal dendritic branches. (*F–H*) Distribution of axonal and dendritic branches. (*F*) Polarized vertebrate neuron, with dendrite/soma compartment carrying postsynaptic sites, and axon compartment with presynaptic sites. (*G*) *Drosophila* type-PD neuron that comes close to the vertebrate pattern, with postsynaptic dendritiform processes concentrated proximally and presynaptic varicose/globular processes distally. (*H*) In *Drosophila* type-C and -D neurons, terminal axons and dendrites are intermingled. Bars, (*B*) 0.5 µm; (*D*) 0.2 µm.

cytoskeleton) and function are similar to the soma and different from the axon (Peters et al. 1976; Baas and Yu 1996). This cell-biological distinction between dendrite/soma and axon goes hand in hand with a functional distinction: Dendrites and soma carry mostly postsynaptic membrane specializations; axons are specialized to conduct axon potentials and carry presynaptic sites at their terminals. The situation is different in insect central neurons. Here, the soma emits a single neurite that in the neuropile forms numerous branches that are dendritic (i.e., postsynaptic), axonal (i.e., presynaptic), or, frequently, mixed (both postsynaptic and presynaptic sites intermingled). For this reason, strictly speaking, one cannot refer to axons or dendrites, but just to neurites, when referring to neuronal processes in the *Drosophila* central nervous system. There clearly exist neurons (those that are part of PD lineages; see Figs. 1I and 4G) that resemble to some extent the typical vertebrate neuron, in the sense that they have postsynaptic (dendritic) branches proximally, close to the soma; a long, unbranched "axon" projects away from these dendrites and ends in multiple axonal terminal branches carrying presynaptic sites. The antennal projection neurons with dendrites in the antennal lobe (primary olfactory center; Stocker 1994; Lai et al. 2008) and axons in the calyx of the MB are an example in this case. But we estimate that the majority of brain lineages are of type C or D: How are presynaptic and postsynaptic sites arranged in neurons belonging to these lineages?

Axiform neurites in any of the microvolumes reconstructed are essentially devoid of synapses. They form the long axon fascicles interconnecting compartments ("macrocircuitry"). These processes then would most closely correspond to the long axons of vertebrates. The swellings of varicose and globular neurites contain almost all presynaptic sites; these then are the terminal axonal branches. The fine processes of dendritiform branches carry postsynaptic

sites. Note that, at least at the level of several microns (which for the 30-µm L1 brain is a lot!), neurites are very predominantly either dendritic or varicose/globular (axonal). This does not mean that a given neuron could not have both types of branches close to each other; but at the level of a given branch, input and output is separated (Fig. 4H). This rule is only violated by the occasional thin "side projections" that occur on or near varicosities and that carry postsynaptic sites contacting nearby presynaptic neurites (see Fig. 6D) (Cardona et al., unpubl.).

MICROCIRCUITRY: DENSITY, BRANCHING, AND DIRECTIONALITY OF NEURITES

The above characterization of neurite ultrastructure applies to all regions sampled so far (six microvolumes: calyx, peduncle periphery, spur, CPL compartment, larval optic neuropile, ventral nerve cord), but there are significant quantitative differences. We summarize findings from three microvolumes: the calyx (input region of MB), spur (output region of mushroom body), and dorsolateral ventral nerve cord.

Afferent axons of the calyx are the antennal projection neurons receiving olfactory input in the antennal lobe (Stocker 1994; Ramaekers et al. 2005). We can identify in the calyx microvolume (Fig. 5A) the largely parallel array of varicose neurites, carrying presynaptic sites, as being derived from the incoming fiber bundle (antenno–protocerebral tract) carrying the antennal projection neurons. In overall volume, varicose/globular afferents comprise ~16% of the neuropile. At a medium diameter of 0.38 µm (reducing the shape of these neurites to smooth cylinders), this corresponds to a density of 4.2 varicose neurites terminating in or passing through a volume of 1 μm^3. Counting the number of branchpoints (for varicose neurites) in the microvolume yields a density of branches at one branch every 4 µm. Presynaptic sites are entirely restricted to the varicose/globular swellings of neurites. We find a density of about four presynaptic sites per 1 μm^3. Forming bundles between the varicose (and globular) presynaptic profiles are the fine terminal fibers of denritiform neurites, mostly derived from MB neurons (Yasuyama et al. 2002). Synapses are mostly dyadic–tetradic, with two to four fine fibers "winding" around swellings of varicose/globular neurites and participating in several synapses. Connectivity is highly local: Individual varicose/globular neurites interact with multiple dendrites in their immediate vicinity.

Neuropile ultrastructure appears to be different in the spur, an output region of the MB (Fahrbach 2006), or the ventral nerve cord. Interestingly, the spur is characterized by the absence of intrinsic glia. Varicose neurites are aligned in bundles that travel along all three cardinal axes (Fig. 5B). Thin terminal filaments of dendritiform neurites are much less frequent than in the calyx (and most other compartments). The lateral connectivity is much more pronounced than in the calyx: If one visualizes all neurites connected to a given synapse, they reach throughout the entire microvolume. Intriguing are also the synaptic geometries: In most cases, two presynaptic sites and two to three postsynaptic sites are clustered together (not shown). We speculate that both wide-field connectivity and multi-input synapses are elements of a microcircuitry required for the specialized function (associative learning) of the MB.

In the dorsolateral domain of the ventral nerve cord (VNC), all neurites are predominantly arranged parallel to the longitudinal axis (Fig. 5C,D). Axonal cable length is 2.9 $\mu m/\mu m^3$ (axiform plus varicose/globular neurites). The branching density is low, with 0.18 branches/1 μm^3. The high quality of the VNC volume allowed us to reconstruct the pattern of thin dendritiform neurites with great confidence. These neurites have a much higher branch density than terminal axons (Fig. 5E,F). As a result, overall dendritic cable length exceeds that of axonal elements by a factor of almost 10. Dendritiform processes show an interesting convergence–divergence pattern (Fig. 5E–H). At a given level, dendritiform processes are not scattered evenly across the section, but they form several bundles of five to ten processes each; one such bundle is highlighted by arrows in Figure 5E,G. Bundles typically run between the loosely packed terminal, varicose axons, with which they form synapses. However, dendrites of a given bundle stay together only for a short interval (<1 µm); subsequently, they diverge and redistribute (compare G and H in Fig. 5), coming together with other dendritform processes in new combinations. This behavior is in contrast to that of axons: Axiform neurites (long axons) form tight bundles where neighborhood relationships among neurites are maintained over many micrometers; terminal varicose/globular axons are more loosely packed, but like axiform processes, they run largely parallel to one another and maintain their position relative to one another (Fig. 5D,G,H).

CONNECTIVITY AND NETWORK MOTIFS IN THE VNC MICROVOLUME

As a result of the high branching density of dendritiform processes, as well as the fact that each presynaptic site contacted multiple postsynaptic profiles, neurites within a microvolume are highly interconnected (as is shown in the proceeding section, this feature distinguishes the *Drosophila* neuropile from a vertebrate brain neuropile). The most common type of network is shown in Figure 6A–C. In the example shown here, one presynaptic element forms two adjacent presynaptic sites on one varicosity. Contacting these sites are six postsynaptic dendritiform processes. Quite frequently, as in this example, a given dendrite contacts its presynaptic partner multiple times at adjacent synapses. Each dendrite forms multiple branches that connect to other presynaptic partners; on average, a dendrite received input from 2.1 axons within the 85-μm^3 VNC microvolume. Figure 6B illustrates the presynaptic element, its associated six postsynaptic elements, and five additional presynaptic elements that are in contact with the same postsynaptic elements. This type of connectivity has been defined as a dense overlapping regulon motif (Reigl et al. 2004; Alon 2007): A given input element diverges onto multiple targets, and at the same time, each target element receives input from multiple presynaptic elements

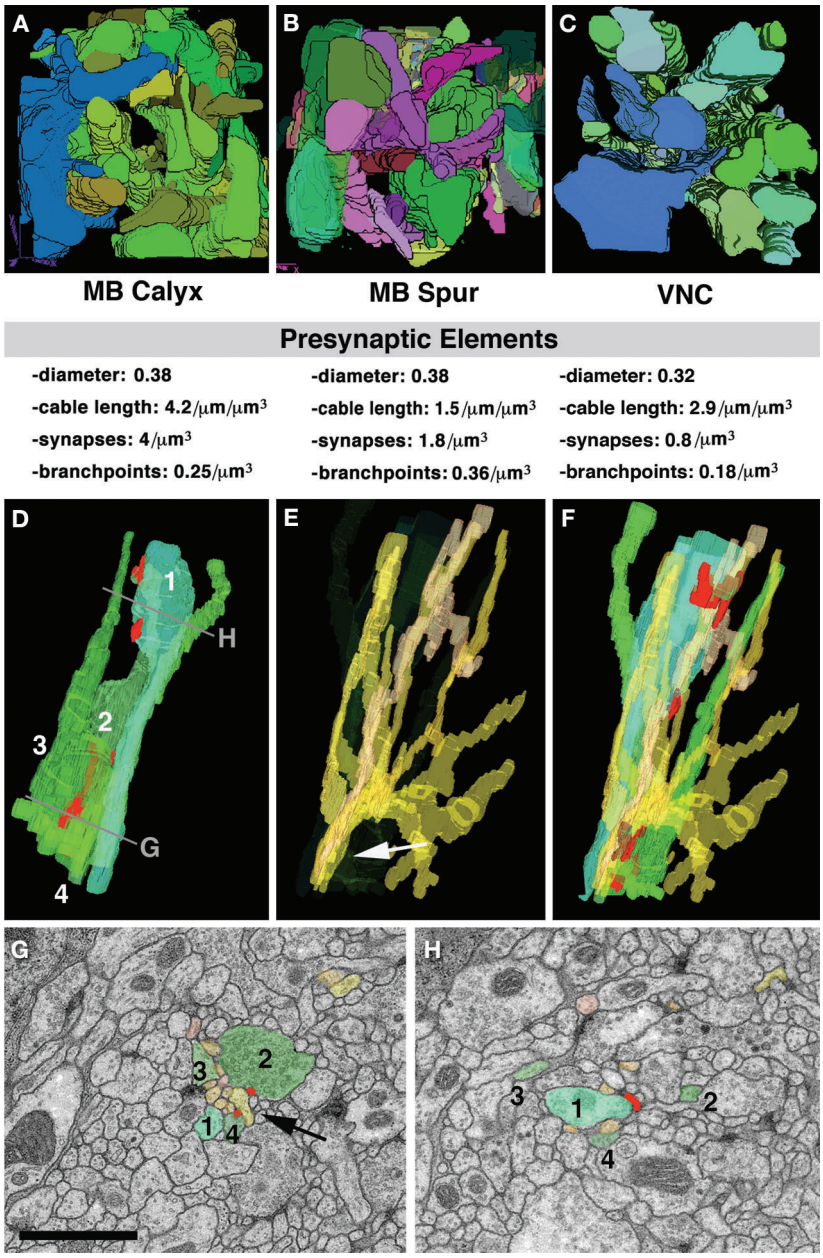

Figure 5. Structural network properties in *Drosophila* brain neuropile. (*A–C*) Three-dimensional digital models of presynaptic varicose/globular neurites from three different microvolumes. (*A,B*) Microvolumes from the calyx (*A*; input region) and spur (*B*; output region) of the MB. In both microvolumes, branches of terminal axonal neurites follow all directions. (*C*) Microvolume from dorsolateral neuropile of the VNC. All neurites are oriented predominantly along the longitudinal axis. Shown below each panel are some core parameters of neurite profiles seen in microvolumes. Note that the average diameter of the presynaptic elements (varicose and globular neurites) is very similar among the different regions. The density of presynaptic sites and branchpoints is significantly lower in the VNC compared to the MB. (*D–H*) Typical trajectories of presynaptic and postsynaptic terminal branches. (*D*) Three-dimensional digital models of four neighboring presynaptic neurites (*1–4*). Neurite *1* has a varicosity near the top of the panel; varicosities of the other neurites are more basal. (*E*) Bundle of dendritiform neurites extending in the vicinity of terminal axons shown in *D*. (*F*) Terminal axons and dendrites shown together. (*G,H*) EM sections close to top and bottom of VNC microvolume (levels of section shown in *D*). Profiles corresponding to the elements shown in models *D–F* are shaded in corresponding colors. As shown here, groups of dendritiform neurites (typically ranging between six and ten) form tight bundles in between adjacent preterminal axons (arrow in *E* and *G*). After forming synaptic contacts, dendritiform neurites typically splay apart (*E*) to then regroup with other dendrites in different configurations. Bar, (*G*), 1 μm.

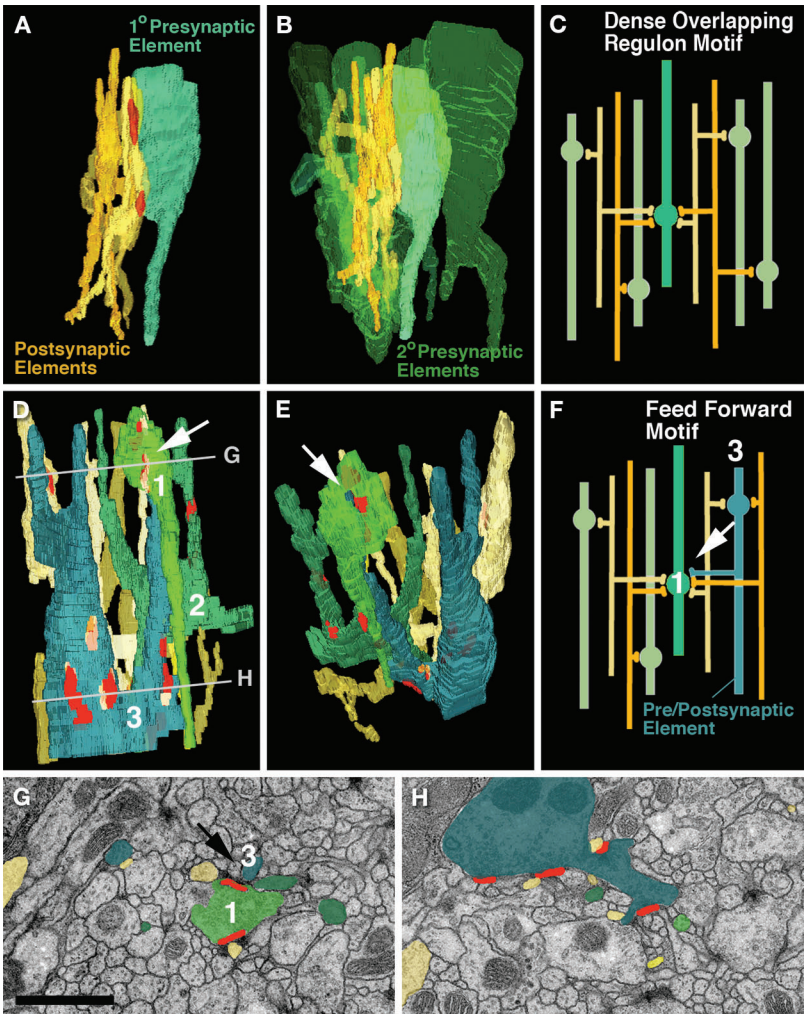

Figure 6. Network motifs that are most frequently encountered in microvolumes. (*A–C*) Dense overlapping regulon motif. (*A*) Segment of one "primary" presynaptic element (turquoise; varicose neurite) that contacts five postsynaptic elements (dendritiform neurites) at two synapses. (*B*) Same configuration of presynaptic and postsynaptic elements as in *A*; shown are several other "secondary" presynaptic elements (green) that form synapses with the same dendrites as the primary axon. (*C*) Schematic representation of this network motif. (*D–H*) Feed forward motif. (*D–F*) Three-dimensional digital models and schematic model of segments of three varicose neurites that form predominantly presynaptic contacts (terminal axons). The blue element has a thin branch that is postsynaptic to the light green element (white arrow in *D–F*). Shown are also the dendritiform postsynaptic neurites that are postsynaptic to both green and blue varicose neurites. (*G,H*) EM sections at levels shown by lines in *D*. *G* represents the top level and shows the synapse between the presynaptic/postsynaptic element (blue) and presynaptic element (green; arrow). Bar, (*G*), 1 µm.

(Fig. 6C). The large majority of presynaptic neurites and postsynaptic neurites within the VNC were engaged in dense overlapping regulon motifs.

Encountered less frequently is a type of connection that we labeled a feed forward motif. An example is shown in Figure 6D–H: Among the postsynaptic partners of one of the varicose neurite (1, light green) are thin branches of two other varicose neurites (2, dark green; 3, blue). In addition, axon A forms input onto several dendrites that at the same time receive input from B and C. In other words, an afferent neurite is at the same time presynaptic to one neurite and postsynaptic to another neighboring neurite; both elements are presynaptic to a common dendritic element. It will be informative to investigate how such network motifs are distributed throughout the brain and how they are correlated to different sensory modalities or types of output.

NEUROPILE ARCHITECTURE IN MAMMALIAN CORTEX AND FLY BRAIN: A FIRST COMPARISON

Quantitative statements about the architecture and connectivity of the neuropile of vertebrate brains, in particular mammalian cortex, were mainly based on statistical analyses of light microscopy preparations (e.g., Golgi-stained prepartions) and representative EM sections (see, e.g., Braitenberg and Schüz 1998). The first reconstruction of a microvolume of mammalian neuropile has recently become available (Mishchenko 2009). What can one learn from the comparison of these data with our data on *Drosophila* larval brain?

Figure 7 presents EM sections of mouse neocortex (A) and *Drosophila* brain (L1 larva, B; adult, C). Plotting the

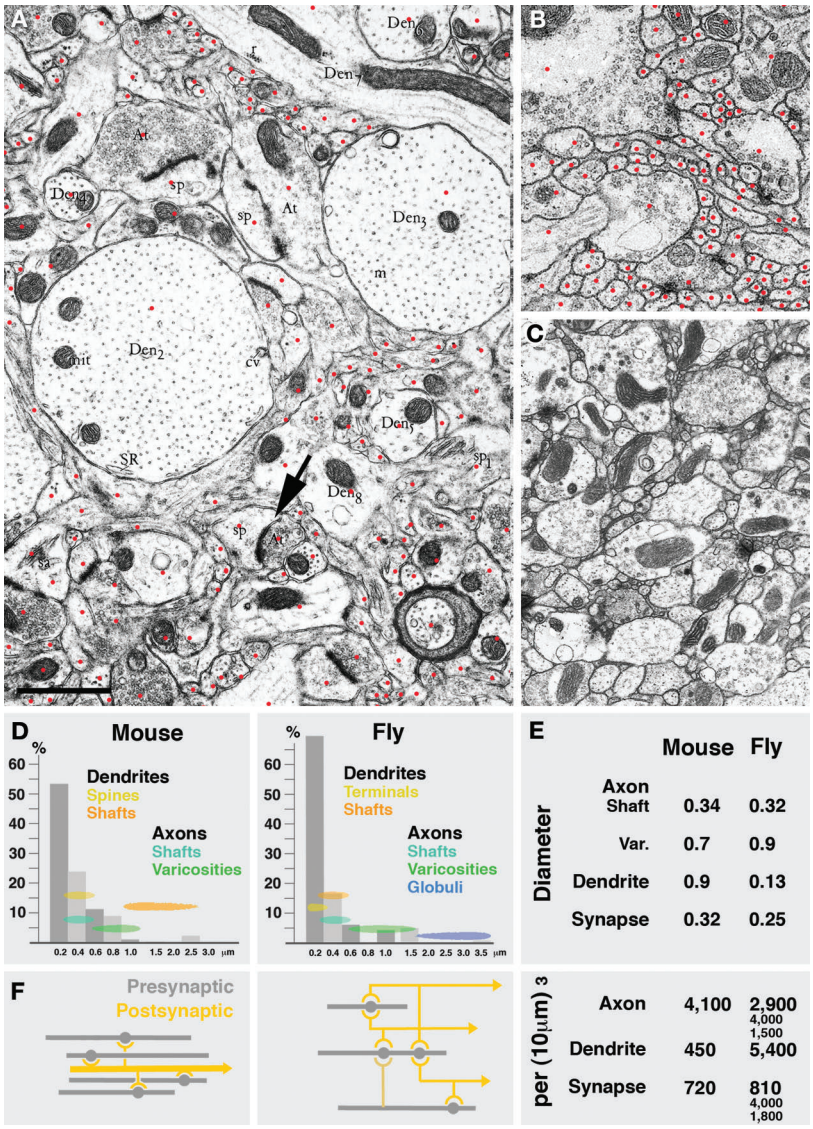

Figure 7. Parameters of microcircuitry in mammalian neocortex and *Drosophila* brain. (*A–C*) Representative EM sections of mouse neocortex (*A*), *Drosophila* larval brain (*B*), and *Drosophila* adult brain (*C*) shown at the same scale. Red dots in the *A* and *B* indicate profiles of individual sectioned neurites. (*D*) Frequency distribution of neurites with different diameters in the mammalian cortex and *Drosophila* brain. Indicated are also the range of diameters that correspond to different neuropile elements (yellow/orange: dendrites; green/blue: axons). (*E*) Comparison of several core parameters in the mouse and *Drosophila* neuropile. In both systems, terminal axons are varicose neurites that form presynaptic sites on their varicosities. Diameters of varicosities are in the range of 0.5–1.5 µm (average in mouse, 0.7 µm; in *Drosophila*; 0.9 µm); the thin segments of terminal axons have an average diameter of ~0.33 µm. The diameter of synapses (presynaptic sites) is also quite similar in both systems (0.32 µm in mammalian cortex, 0.25 µm in fly brain). The overall cable length of terminal axons per volume unit is also comparable: 4100 µm per 1000 µm^3 in mouse and between 1500 µm and 4,000 µm in different microvolumes of fly brain. The major difference between the mouse and fly neuropile lies in the size and branching density of dendrites. In *Drosophila*, dendrites are very thin (average diameter: 0.13 µm) and densely branched; in mammalian brain, dendrites are thick (average diameter: 0.9 µm; see even thicker examples of dendrites in *A*) and branches are much further apart. This is also reflected in the dendritic cable length, which is 450 mm/1000 µm^3 in mouse and more than 10-fold higher in *Drosophila*. Lower branch density as well as the absence of polyadic synapses in mouse cortex neuropile also results in a considerably less dense connectivity, schematically shown in *F*. Shown for *Drosophila* is the dense overlapping regulon motif, in which the large majority of neurite segments encountered in any microvolume of 100 µm^3 or more is engaged. In a mammalian cortical microvolume of that size, dendrite segments are unbranched; the only type of connectivity is convergence, whereby multiple terminal axons converge on a dendritic segment that happens to be within their range. Bar, (*A*), 1 µm.

frequency of profiles with different diameters shows quite similar distributions in mouse and fly (Fig. 7D). In particular, the average diameter of axon shafts and synapse-bearing varicosities, as well as presynaptic sites themselves, is quite conserved. The most conspicuous difference between the two species lies in the size of dendrites. In mouse cortex, dendrite shafts are large, measuring in average almost 1 µm (Fig. 7D,E) (Braitenberg and Schüz 1998). Many dendrites are considerably thicker (e.g., examples shown in Fig. 7A). Dendrites of pyramidal cells (and some other classes of neurons) bear spines, which are club-shaped processes of 1–2 µm in length with an average diameter of ~0.4 µm. Synapses are found on dendritic shafts and spines; synapses are typically monadic, which naturally follows from the fact that the presynaptic element is of equal size, or even smaller, than the postsynaptic element (arrow in Fig. 7A). The comparison between the mouse and fly in regard to axonal and dendritic cable length per volume unit is also informative (Fig. 7E). In the mouse, axonal cable adds up to ~4 mm/1000 μm^3; the length of dendrites is 0.5 mm. Axonal cable length in *Drosophila* lies in the same range; dendritic cable length, on the other hand, is 10 times higher, which is a reflection of the fact that dendritic processes are very thin and highly branched. Interestingly, judging from the inspection of EM photographs (see, e.g., Peters et al. 1976), processes in the 0.1-µm range seem to be quite numerous also in mammalian brain, but the nature of these thin neurites is unclear.

As described in the previous section, the overall synaptic density per volume unit seems to be quite different in different parts of the fly brain, ranging from ~1/μm^3 (VNC) to >4/μm^3 (input region of MB). In the mammalian cortex, synaptic density is toward the lower end of this range, at 0.72/μm^3 (Braitenberg and Schüz 1998). Approximately the same value was extracted from the microvolume of rat hippocampus (Chklovskii et al., unpubl.). Here, one axonal varicosity typically contained a single synapse; in *Drosophila*, most varicosities had between two and four synaptic sites. The higher density of synapses in *Drosophila* is accompanied by a higher number of branchpoints. In the rat hippocampus microvolume, measuring 8 x 8 x 8 µm, very vew axons or dendrites (out of hundreds) had any branches, not counting dendritic spines. Similarly, statistical analysis of Golgi preparations yielded typical distances of 10 µm and higher between branchpoints (Braitenberg and Schüz 1998). In contrast, in *Drosophila*, terminal axons had one branchpoint every 4 µm (MB calyx), 2.8 µm (MB, spur) or 7.5 µm (VNC), respectively. Dendritic branch density is even higher; in the VNC microvolume, dendritiform neurites had approximately twice as many branchpoints as varicose/globular neurites.

The fact that the spacing of branches and synapses is significantly higher in the *Drosophila* brain compared to the mammalian brain is reflected in the presence of a much higher connectedness of neurites in the former. As described in the previous section, the majority of axons are engaged in networks containing both dendrites and other axons within a microvolume of less than 100 μm^3. This is not the case in mammalian microvolumes of comparable, or even larger, size (Chklovskii et al., unpubl.). Here, the only type of connectivity is represented by a convergence of axonal segments onto isolated dendritic segments (Fig. 7H). However, unlike the fly brain, very few axonal segments will form input to more than one dendrite, so that network motifs such as the dense overlapping regulon motif or feed forward motif do not emerge. What this simply means is that the modules of mammalian brain that house microcircuits are considerably larger than those in *Drosophila*. In vertebrates, neurons reach much higher numbers than in the *Drosophila* brain. Furthermore, dendrites are larger in diameter, and polyadic synapses are largely absent. This results in connectivity occupying more space: in *Drosophila*, one presynaptic neurite reaches up to six postsynaptic elements in a single synapse. In mammalian brain, for the same purpose, six individual synapses, spaced apart by intervals of several micrometers, would have to be formed. One may speculate that, evolutionarily, each neuron grew in axonal and dendritic length to accommodate the higher number of synapses that had to form to connect a given neuron to a certain fraction of other neurons. As a result of this numerical increase in cell number, cable length, and synapse number, branches of dendrites and axons are spaced much further apart, such that in a volume of 8 x 8 x 8 µm almost no branchpoints (and consecutively no networks) occur.

A GLIMPSE AT THE PHYLOGENY OF NEUROPILE ARCHITECTURE

Systematic studies of neuropile architecture and connectivity from serial EM sections have not been performed for other animals, with the exception of the central nervous system of the nematode *C. elegans* (White et al. 1986). On the other hand, there is a rich literature documenting neurites and synapses in representative EM sections. These neuropile elements exist in all metazoans. Measurements of diameters of neurites and synapses, taken from representative photographs published in the literature (mollusk: Nagy and Elekes 2000; annelid: Riehl and Schlue 1998; vertebrate: Peters et al. 1976; nematode: White et al. 1986; acoela: our material) yielded figures similar to those for *Drosophila*. Presynaptic sites measured 0.2–0.35 µm in diameter. Neurite numbers, as in *Drosophila*, showed a peak in the range below 0.2 µm in diameter. In addition, a substantial number of neurites were in the range of 0.4–0.8 µm. Presynaptic sites are typically located on profiles with a diameter of 0.4–0.8 µm; these presynaptic sites contact a variable number of thin postsynaptic dendrites. Large profiles serving as postsynaptic sites (as in vertebrates) are rarely reported. This finding, which should be substantiated with further systematic serial reconstruction of microvolumes, suggests that the pattern of neurites shown here for *Drosophila*, with thin highly branched dendrites that engage with medium-sized varicose axons through polyadic synapses, may be primitive. The appearance of "gigantic" dendrites, accompanied by a significant increase in the number of neurons and overall cable length, appears to be an innovation of the vertebrate clade.

C. elegans with its miniaturized central nervous system, consisting of less than 400 neurons, presents an interesting case with respect to neuropile architecture. Thin profiles below 0.2 µm are almost entirely absent; the large majority of neurites have a diameter of 0.3–0.6 µm. This anomaly among invertebrate taxa is accompanied by the fact that neurons of *C. elegans* are almost all unbranched (White et al. 1986). Most somata project a single neurite that carries clusters of intermingled presynaptic and postsynaptic sites. In other words, thin terminal dendritiform branches as in other taxa do not exist in the worm.

OUTLOOK

We propose that the 3D reconstruction of neuropile architecture and connectivity will provide an important tool for the study of brain function and development. The technology we present here is well adapted to handle small volumes of neuropile, but a number of technical improvements are under way that will bring larger volumes (in the size range of adult fly brains) into the range of feasibility. The improvements are directed at three major bottlenecks of the procedure: better registration, automatic segmentation, and automatic feature extraction. Programs in the trial phase allow for automatic recognition of profile boundaries and subsequent segmentation (Chklosvskii et al., unpubl.). A step in microvolume analysis that is currently as labor-intensive as segmentation (which takes 5–10 working days per volume) is extracting relevant information from the segmented objects. For example, we currently manually input what synapse belongs to what neurite and manually generate lists that encapsulate the connectivity pattern. We are working on adding features to the EM canvas window that fully automate these tasks. Thus, after segmentation of neurite profiles, synapses can be assigned automatically to the underlying 3D reconstructed neuronal arborizations that host them. With not much extra effort than merely segmentation, a complete wiring diagram of the microvolume can be built. The next step would be to generate dynamic models, where lengths and diameters of neurites, intersynapse distances, and other parameters are taken into account to predict the temporal component of activity flow. We anticipate that these models of small volumes will provide suitable material for computational neuroscientists to build more accurate and heuristically valuable large-scale models of brain function.

ACKNOWLEDGMENTS

We thank many friends and collaborators, notably Dmitrii Chklovskii, Johannes Schindelin, James Truman, and Wayne Pereanu, for helpful discussions and comments. Parts of this work were supported by National Institutes of Health grant R01 NS054814 to V.H.

REFERENCES

Alon U. 2007. Network motifs: Theory and experimental approaches. *Nat Rev Genet* **8:** 450–461.

Baas PW, Yu W. 1996. A composite model for establishing the microtubule arrays of the neuron. *Mol Neurobiol* **12:** 145–161.

Braitenberg V, Schüz A. 1998. *Cortex: Statistics and geometry of neuronal connectivity,* 2nd ed. Springer, Berlin.

Brand AH, Perrimon N. 1993. Targeted gene expression as a means of altering cell fates and generating dominant phenotypes. *Development* **118:** 401–415.

Douglas R, Martin KAC. 1998. Neocortex. In *The synaptic organization of the brain* (ed. GM Shepherd), pp. 459–511. Oxford University Press, NY.

Fahrbach SE. 2006. Structure of the mushroom bodies of the insect brain. *Annu Rev Entomol* **51:** 209–232.

Feeney CJ, Karunanithi S, Pearce J, Govind CK, Atwood HL. 1998. Motor nerve terminals on abdominal muscles in larval flesh flies, *Sarcophaga bullata:* Comparisons with *Drosophila*. *J Comp Neurol* **402:** 197–209.

Fung S, Wang F, Spindler S, Hartenstein V. 2009. *Drosophila* E-cadherin and its binding partner Armadillo/β-catenin are required for axonal pathway choices in the developing larval brain. *Dev Biol* **332:** 371–382.

Goodman CS, Doe CQ. 1993. Embryonic development of the *Drosophila* central nervous system. In *The Development of* Drosophila (ed. M Bate and A Martinez-Arias), pp. 1131–1206. Cold Spring Harbor Laboratory Press, Cold Spring Harbor, NY.

Hartenstein V, Spindler S, Pereanu W, Fung S. 2008a. The development of the *Drosophila* larval brain. *Adv Exp Med Biol* **628:** 1–31.

Hartenstein V, Cardona A, Pereanu W, Younossi-Hartenstein A. 2008b. Modeling the developing *Drosophila* brain: Rationale, technique and application. *BioScience* **58:** 823–836.

Ito K, Awano W, Suzuki K, Hiromi Y, Yamamoto D. 1997. The *Drosophila* mushroom body is a quadruple structure of clonal units each of which contains a virtually identical set of neurones and glial cells. *Development* **124:** 761–771.

Kaneko M, Hall JC. 2000. Neuroanatomy of cells expressing clock genes in *Drosophila:* Transgenic manipulation of the *period* and *timeless* genes to mark the perikarya of circadian pacemaker neurons and their projections. *J Comp Neurol* **422:** 66–94.

Kittel RJ, Wichmann C, Rasse TM, Fouquet W, Schmidt M, Schmid A, Wagh DA, Pawlu C, Kellner RR, Willig KI, et al. 2006. Bruchpilot promotes active zone assembly, Ca^{2+} channel clustering, and vesicle release. *Science* **312:** 1051–1054.

Kozloski J, Hamzei-Sichani F, Yuste R. 2001. Stereotyped position of local synaptic targets in neocortex. *Science* **293:** 868–872.

Lai SL, Awasaki T, Ito K, Lee T. 2008. Clonal analysis of *Drosophila* antennal lobe neurons: Diverse neuronal architectures in the lateral neuroblast lineage. *Development* **135:** 2883–2893.

Larsen C, Shy D, Spindler S, Fung S, Younossi-Hartenstein A, Hartenstein V. 2009. Patterns of growth, axonal extension and axonal arborization of neuronal lineages in the developing *Drosophila* brain. *Dev Biol* **335:** 289–304.

Meinertzhagen IA, O'Neil SD. 1991. Synaptic organization of columnar elements in the lamina of the wild type in *Drosophila melanogaster*. *J Comp Neurol* **305:** 232–263.

Michchenko Y. 2009. Automation of 3D reconstruction of neural tissue from large volume of conventional serial section transmission electron micrographs. *J Neurosci Methods* **176:** 276–289.

Nagy T, Elekes K. 2000. Embryogenesis of the central nervous system of the pond snail *Lymnea stagnalis* L. An ultrastructural study. *J Neurocytol* **29:** 43–60.

Pereanu W, Hartenstein V. 2006. Neural lineages of the *Drosophila* brain: A 3D digital atlas of the pattern of lineage location and projection at the late larval stage. *J Neurosci* **26:** 5534–5553.

Pereanu W, Jennett A, Younossi-Hartenstein A, Hartenstein V. 2009. A development-based compartmentalization of the *Drosophila* central brain. *J. Comp. Neurol*. (in press).

Peters A, Palay S, Webster HE. 1976. *The fine structure of the nervous system*. W.B. Saunders, Philadelphia.

Prokop A, Meinertzhagen IA. 2006. Development and structure of synaptic contacts in *Drosophila*. *Semin Cell Dev Biol* **17:** 20–30.

Ramaekers A, Magnenat E, Marin EC, Gendre N, Jefferis GS, Luo L, Stocker RF. 2005. Glomerular maps without cellular redundancy at successive levels of the *Drosophila* larval olfactory circuit. *Curr Biol* **15:** 982–992.

Reigl M, Alon U, Chklovskii DB. 2004. Search for computational modules in the *C. elegans* brain. *BMC Biol* **2:** 2–25.

Riehl B, Schlue WR. 1998. Morphological organization of neuropile glial cells in the central nervous system of the medicinal leech (*Hirudo medicinalis*). *Tissue Cell* **30:** 177–186.

Rolls ET, Loh M, Deco G, Winterer G. 2008. Computational models of schizophrenia and dopamine modulation in the prefrontal cortex. *Nat Rev Neurosci* **9:** 696–709.

Saalfeld S, Cardona A, Hartenstein V, Tomancák P. 2009. CATMAID: Collaborative annotation toolkit for massive amounts of image data. *Bioinformatics* **25:** 1984–1986.

Silberberg G. 2008. Polysynaptic subcircuits in the neocortex: Spatial and temporal diversity. *Curr Opin Neurobiol* **18:** 332–337.

Silberberg G, Gupta A, Markram H. 2002. Stereotypy in neocortical microcircuits. *Trends Neurosci* **25:** 227–230.

Stocker RF. 1994. The organization of the chemosensory system in *Drosophila melanogaster:* A review. *Cell Tissue Res* **275:** 3–26.

Toledo-Rodriguez M, El Manira A, Wallén P, Svirskis G, Hounsgaard J. 2005. Cellular signalling properties in microcircuits. *Trends Neurosci* **28:** 534–540.

Truman JW, Schuppe H, Shepherd D, Williams DW. 2004. Developmental architecture of adult-specific lineages in the ventral CNS of *Drosophila. Development* **131:** 5167–5184.

Urbach R, Technau GM. 2003. Molecular markers for identified neuroblasts in the developing brain of *Drosophila*. *Development* **130:** 3621–3637.

Watson AH, Burrows M. 1983. The morphology, ultrastructure, and distribution of synapses on an intersegmental interneuron of the locust. *J Comp Neurol* **214:** 154–169.

White JG, Southgate E, Thomson JN, Brenner S. 1986. The structure of the nervous system of the nematode *Caenorhabditis elegans. Philos Trans R Soc Lond B* **314:** 1–340.

Winterer G, Weinberger DR. 2004. Genes, dopamine and cortical signal-to-noise ratio in schizophrenia. *Trends Neurosci* **27:** 683–690.

Yasuyama K, Meinertzhagen IA, Schürmann FW. 2002. Synaptic organization of the mushroom body calyx in *Drosophila melanogaster. J Comp Neurol* **445:** 211–226.

Younossi-Hartenstein A, Nassif C, Green P, Hartenstein V. 1996. Early neurogenesis of the *Drosophila* brain. *J Comp Neurol* **370:** 313–329.

Younossi-Hartenstein A, Salvaterra P, Hartenstein V. 2003. Early development of the *Drosophila* brain. IV. Larval neuropile compartments defined by glial septa. *J Comp Neurol* **455:** 435–450.

Younossi-Hartenstein A, Shy D, Hartenstein V. 2006. The embryonic formation of the *Drosophila* brain neuropile. *J Comp Neurol* **497:** 981–998.